Optical Engineering

OpticalEngineering.SPIEDigitalLibrary.org

Performance validation on an all-fiber 1.54-μm pulsed coherent Doppler lidar for wind-profile measurement

Heng Liu
Lucheng Yuan
Chunhui Fan
Feifei Liu
Xin Zhang
Xiaopeng Zhu
Jiqiao Liu
Xiaolei Zhu
Weibiao Chen

SPIE.

Heng Liu, Lucheng Yuan, Chunhui Fan, Feifei Liu, Xin Zhang, Xiaopeng Zhu, Jiqiao Liu, Xiaolei Zhu, Weibiao Chen, "Performance validation on an all-fiber 1.54-μm pulsed coherent Doppler lidar for wind-profile measurement," *Opt. Eng.* **59**(1), 014109 (2020), doi: 10.1117/1.OE.59.1.014109

Performance validation on an all-fiber 1.54-μm pulsed coherent Doppler lidar for wind-profile measurement

Heng Liu,[a,b] Lucheng Yuan,[a,b] Chunhui Fan,[c] Feifei Liu,[a] Xin Zhang,[a] Xiaopeng Zhu,[a,b,*] Jiqiao Liu,[a,b] Xiaolei Zhu,[a,b,*] and Weibiao Chen[a,b]

[a]Chinese Academy of Science, Shanghai Institute of Optics and Fine Mechanics, Key Laboratory of Space Laser Communication and Detection Technology, Shanghai, China

[b]University of Chinese Academy of Sciences, Center of Materials Science and Optoelectronics Engineering, Beijing, China

[c]National University of Defense Technology, College of Meteorology and Oceanography, Nanjing, China

Abstract. The characteristics and capability of a homemade all-fiber 1.54-μm pulsed coherent Doppler lidar (CDL) were validated in field experiments by comparing the detection results with a collocated lidar and sounding balloons. With the range gate of 30 m and temporal resolution of 16 s at velocity–azimuth display mode, the detection capability of the CDL ranged from 0.1 to 5 km, and the time sequence and height position of this CDL were calibrated by the collocated lidar. In the intercomparison experiments with sounding balloons, the discrepancy of 30-s averaged measurement results of horizontal wind speed and wind direction was nearly 0.7 m/s and 5.3 deg, respectively. The good agreement achieved in such a short averaged time period was a convincing case of intercomparison experiments between CDL and sounding balloon. The CDL system demonstrated good reliability and operational stability in field experiments.
 [DOI: 10.1117/1.OE.59.1.014109]

Keywords: all-fiber; coherent Doppler lidar; wind profile; field experiments; intercomparison; sounding balloons.

Paper 191580 received Nov. 8, 2019; accepted for publication Dec. 24, 2019; published online Jan. 21, 2020.

1 Introduction

Coherent Doppler lidar (CDL) has been developed as a powerful tool for atmospheric wind velocity measurement,[1–4] aircraft wake-vortex hazard detection,[5–7] and wind turbulence measurement[8,9] with high temporal space resolution and high measurement accuracy due to its high carrier-to-noise detecting characteristics. The enabling modules for high-performance CDL system include laser transmitter,[10–12] balanced detection,[13,14] and weak-regime wind estimation algorithm.[15,16] Adopting a single longitudinal mode laser and a balanced detector is helpful for a CDL to realize high signal-to-noise ratio (SNR). Recently, all-fiber 1.5-μm pulsed CDL has attracted much attention due to its eye safety, compactness, flexible deployment, and mature fiber components from telecommunication industry.[17]

The performance of CDL has been proved by intercomparison experiments with reliable wind measurement instruments in the past dozen years. The first high pulse energy CDL (~100 mJ at 2-μm wavelength) was developed by NASA Langley Research Center; it was used as a calibration and validation lidar (so-called "Validar"),[18] and the intercomparison results with ground-based wind-observing lidar facility were so encouraging.[19] Mitsubishi Electric Corporation developed an airborne 1.5-μm pulsed CDL, which was capable of detecting as far as 9.3 km with modifiable range resolutions, and the wind velocity measurement accuracy of the prototype was inspected in comparison with L-band wind profiler.[20–22] In 2011, Leosphere displayed a long-range lidar (Windcube 200S), which could measure three-dimensional (3-D)

*Address all correspondence to Xiaopeng Zhu, E-mail: xp_zhu@siom.ac.cn; Xiaolei Zhu, E-mail: xlzhu@siom.ac.cn

wind profiles up to 7 km in distance with 70-m range resolution, and the radial velocity with 0.5-m/s velocity resolution was validated by another lidar (Windcube 70).[23] In 2016, Zhai et al.[24] developed a 1.5-μm pulsed CDL with variable spatial resolution from 15 to 60 m; its discrepancies with radiosonde observation results were within acceptable limits. In 2017, Wang et al.[3] presented a versatile CDL with 0.5-m/s measurement precision and 6-km detection ability, and its stability was demonstrated by continuous wind detection of the atmospheric boundary layer. According to the Commission for Instruments and Methods of Observation guidebook,[25] the accuracy of high-quality windfinding systems should be maintained in less than wind speed of 1 m/s and direction of 5-deg level. In view of the accuracy requirement of windfinding systems, the averaging time period in the intercomparison experiment was set to 30,[26] 15,[4] 3 min,[27] etc.

In this work, an all-fiber 1.54-μm pulsed CDL with high pulse energy (300 μJ/pulse) laser at repetition rate of 10 kHz was developed for measuring wind profiles. Dozens of sounding balloons and a collocated lidar were used to verify the reliability and stability of the CDL. The wind measurement capability of the homemade CDL was verified by the sounding balloons with the time and space interval of merely 30-s and 30-m levels, respectively. To our knowledge, the relatively short averaged time is a convincing case for wind measurement by CDL compared with sounding balloons.

2 Methodology

2.1 *Pulsed CDL System*

The pulsed CDL transmits narrow bandwidth laser pulses into the atmosphere, and then the line of sight (LOS) wind velocity can be acquired by calculating the Doppler shift caused by moving aerosols. This pulsed CDL system is mainly composed of high-energy single-frequency pulsed laser source, optical antenna system, highly sensitive heterodyne detector, signal acquisition, and real-time processing section. The system diagram is shown in Fig. 1.

The pulsed laser unit is a master oscillator power amplification system, and the seeder laser is a distributed feedback single-frequency continuous wave laser.[12] The seeder laser beam is divided into two parts by a 1×2 optical fiber splitter. One part (about 0.8 mW) is used as the local oscillator (LO) for heterodyne detection, and the other part is pulse modulated and frequency (intermediate frequency: 160 MHz) shifted by an acousto-optic modulator. The laser pulse was amplified by multistage optical fiber amplifiers and finally up to 300-μJ pulse energy output with

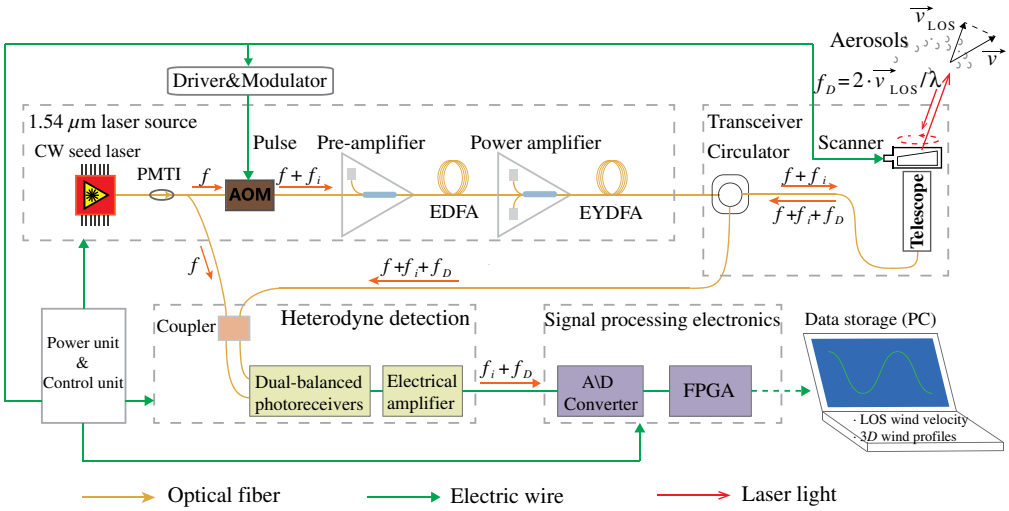

Fig. 1 System diagram of the pulsed CDL (PMTI, polarization-maintaining tap isolator; AOM, acousto-optical modulators; EDFA, erbium-doped fiber amplifier; EYDFA, erbium–ytterbium codoped fiber amplifier; FPGA, field programmable gate array).

pulse duration of 400 ns at 10-kHz pulse repetition rate was obtained. The central wavelength was 1540 nm.[17]

The optical antenna system is mainly composed of a fiber optical circulator, a coaxial telescope, and a scanner. The fiber circulator is applied to insulate transmitting laser beam and backscattered signal from aerosols. The outgoing laser beam goes into telescope from the output port of the circulator, and then is collimated to 80 mm in diameter. The effective aperture of the telescope is 100 mm. The scanner is used to realize velocity–azimuth display (VAD) scanning by rotating one optical wedge with elevation angle of 20 deg. The LOS wind speeds detected from eight azimuths are used to retrieve the wind vector within 16 s.

The highly sensitive heterodyne detector is used to detect the frequency beating signal caused by mixing the backscattered signal and the LO beam. The frequency beating signal is obtained using a 2×2 (50:50) single-mode polarization-maintaining fiber coupler. The heterodyne signal is sampled by an acquisition card with 1 GSPS sampling rate with 10 bits resolution. The total sampling time is about 40 μs, which is divided into 200 time gates, corresponding to 30-m space–distance per time gate. Fast Fourier transform (FFT) and power spectrum accumulations are implemented in every time gate. The power spectra are finally sent to a computer via RS422 interface, and the LOS wind velocity can be obtained by the traditional peak detection method. The main parameters of the CDL system are listed in Table 1.

To extract the peak value of the power spectra corresponding to the Doppler shift, gravity method is used here, and the LOS wind velocity can be expressed as[4]

$$v_{\mathrm{LOS}}^{g} = \frac{\lambda}{2}\left(\frac{f_s}{N} \cdot \frac{\sum_{x=N_x-F/2}^{N_x+F/2} x \cdot P_s(f_x)}{\sum_{x=N_x-F/2}^{N_x+F/2} P_s(f_x)} - f_{\mathrm{IF}}\right), \tag{1}$$

where λ is the laser wavelength, f_s is the sampling rate, N is the total number of FFT points, P_s is the amplitude of the point in the width of power spectra, N_x is the peak value location of the power spectra, F is the integration window width, and f_{IF} is the intermediate frequency. The integration window width here is approximately set to be 6 MHz.[28]

The multiazimuth LOS wind velocities usually have the sine function in VAD scanning mode, which is applied to eliminate the exceptional points and reduce random error. The 3-D wind profiles can be rebuilt by

$$v_{\mathrm{LOS}} = u(z)\sin\theta\sin\varphi + v(z)\cos\theta\sin\varphi + w(z)\cos\varphi, \tag{2}$$

Table 1 Main parameters of the pulsed CDL system.

Component	Qualification	Specification
Transmitter (seeder: RIO Inc. RIO0099-XX)	Operating wavelength	1540 nm
	Pulse energy	300 μJ
	Pulse repetition rate	10 kHz
	Pulse width	400 ns
Transceiver (homemade)	Scan	VAD mode
	Zenith angle	20 deg
	Number of azimuth	8
	Scanning period	16 s
Acquisition card (AD: ADS5400)	Sampling rate	1 GSPS
	Resolution	10 bits ADC
	Range gate	30 m
	Total sampling time	40 μs

$$v_h = \sqrt{u^2 + v^2}, \tag{3}$$

where u, v, and w are the x, y, and z axial projection of wind vector, respectively, θ is the azimuth angle, and φ is the elevation angle.

2.2 *Calibration Method of Wind Velocity between Collocated Lidar and the CDL*

The collocated lidar (Molas B300), scaled by German WindGuard testing organization, is a Doppler lidar with distance detection range of 40 to 300 m and wind velocity detection range of 0 to 60 m/s. The accuracy of 10-min averaged wind speed and direction is 0.1 m/s and 1 deg, respectively.

Molas B300 can detect from 40 to 260 m in distance with range gate of 20 m, and its zenith angle is 28 deg. Considering the distance detection range of 0.1 to 5 km for our CDL, it is believed that the wind velocity in range of 100 to 260 m is suitable for calibration.

Molas B300 can export both 1-s and 10-min averaged wind speed dataset, and the 1-s dataset can be utilized in time and height matching with the CDL. On the basis of correct time sequence and similar height, the comparison results of 10-min averaged wind profiles can be obtained.

2.3 *Comparative Method for Horizontal Wind Velocity between Sounding Balloon and the CDL*

Sounding balloon can directly detect wind vector by tracking the balloon with Beidou/GPS navigation module. The dataset from sounding balloon includes 30-s averaged horizontal wind velocity with 1-s updating period. Its measurement repeatability of the 30-s averaged wind speed and direction of sounding balloon is about 0.2 m/s and 2 deg, respectively.[29,30] The vertical range resolution is about 5 m in both ascent and descent periods.

The comparison data from sounding balloon and the CDL should also be matched at time and altitude. Since the horizontal distance between starting point of sounding balloon and the CDL is <50 m, the wind measured by sounding balloon is identified as the wind field detected by the CDL. The comparative scheme of horizontal wind velocity based on the time and altitude characteristics of these two instruments are listed in Table 2.

3 Results and Discussions

In August 2018, concurrent measurements of sounding balloons and Molas B300 were implemented in Jingbian City, Shanxi Province. During the field experiments, every sounding balloon was released once the last one's detection had been finished, and the local time displayed the recorded time zone of the ground-based CDL, as shown in Table 3.

Tracks of sounding balloons and relative positions of the two instruments are displayed in Fig. 2. The altitude of the sounding balloon covers both ascent and descent periods reflected by the colored curves. Their locations corresponded to the coordinates could roughly indicate the horizontal wind direction.

Table 2 Comparative scheme of horizontal wind velocity.

	Temporal resolution (s)	Dataset updating time (s)	Altitude interval (m)
Sounding balloon	30	1	~5
CDL	16	2	30
Comparison	30	~1	30

Table 3 Summary of field experiments.

No.	Date	Local time		Altitude (m)	Instrument
		Start	Stop		
1	August 1, 2018	12:50	1:28 am	1332	CDL, balloon, Molas B300
2	August 10, 2018	12:46	1:23 am	1332	CDL, balloon, Molas B300
3	August 15, 2018	18:04	21:51	1332	CDL, balloon, Molas B300

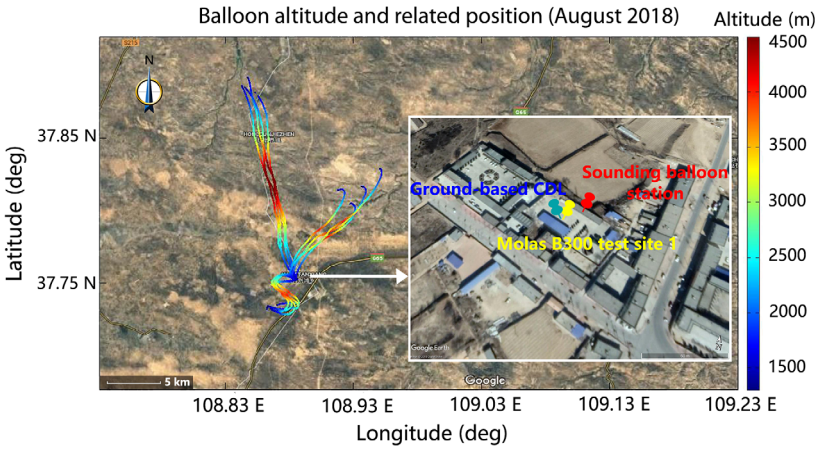

Fig. 2 An overview of the field sites. Tracks of sounding balloon are shown in colored curves. Related positions of sensors are marked on the right inset.

3.1 *Calibration of the CDL*

To calibrate the wind vector measured by the CDL, Molas B300 was set in campaign. The similar outline of 1-s level wind velocity of both Molas B300 and the CDL reflects correct time and height matching of two lidars. To eliminate random error and utilize the secondary datasets (10-min averaged wind velocity of Molas B300), the 10-min averaged wind velocity of two lidars are compared and similar tendency is obtained and plotted in Fig. 3. The time and height matching of two lidars shows good accordance after time–height matching.

Statistics analysis of measured vertical wind velocity between the CDL and Molas B300 is shown in Fig. 4. The correlation coefficients (R: 0.964 of horizontal wind speed, 0.992 of horizontal wind direction, and 0.963 of vertical wind velocity) revealed a significant correlation between two lidar datasets. The discrepancy of 10-min averaged horizontal wind speed and direction is 0.164 m/s and 1.719 deg, respectively. The standard deviation of those two kinds of 10-min averaged vertical velocity is decreased to 0.076 m/s. The bias is −0.069 m/s, which reveals a systematic bias due to the intermediate frequency shift. The sample of horizontal wind speed profile also displays high similarity as shown in Fig. 4(d). These results provide the calibration accuracy of the CDL.

3.2 *Intercomparison Experiments of the CDL and Sounding Balloons*

The time–altitude matching comparison of horizontal wind velocity between the CDL and sounding balloon, including ascent and descent periods, is presented in Fig. 5. The overall similarity of wind velocity of two sensors emerges while tiny distinction exists inevitably. The common discrepancy of horizontal wind speed of two sensors is <1 m/s. The 10-min error bar is attached to the measurement dataset of our CDL. At altitude from 1500 to 3000 m, the error bar is so short due to the high SNR and relatively steady wind field. In the weak detection regime, the error bar increases with low SNR. However, the central measurement data retrieved from the CDL is still close to the measurement data of sounding balloons. The accuracy of the CDL is

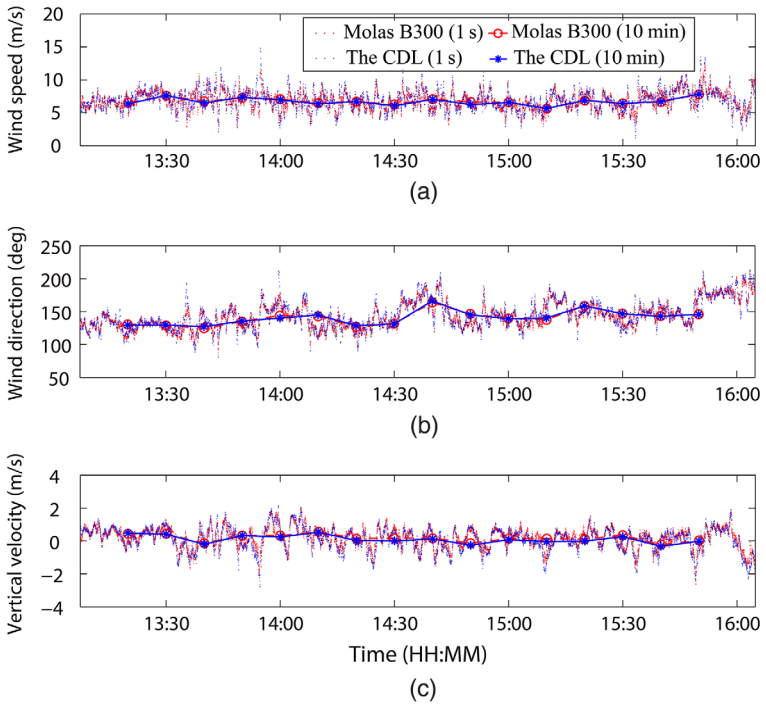

Fig. 3 Calibration of the CDL by Molas B300 (sample at 165-m height). (a) Horizontal wind speed calibration of the CDL, (b) horizontal wind direction calibration of the CDL, and (c) vertical wind velocity calibration of the CDL.

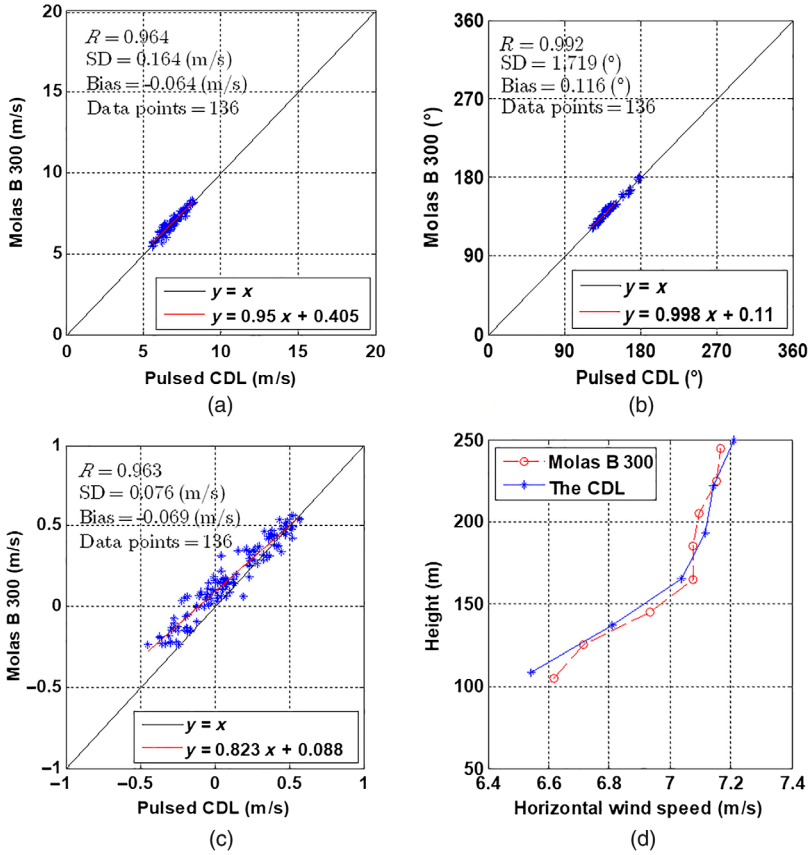

Fig. 4 Statistic analysis of 10-min averaged wind velocity measured by Molas B300 and the pulsed CDL. (a) Horizontal wind speed correlation, (b) horizontal wind direction correlation, (c) vertical wind velocity correlation, and (d) horizontal wind speed profile.

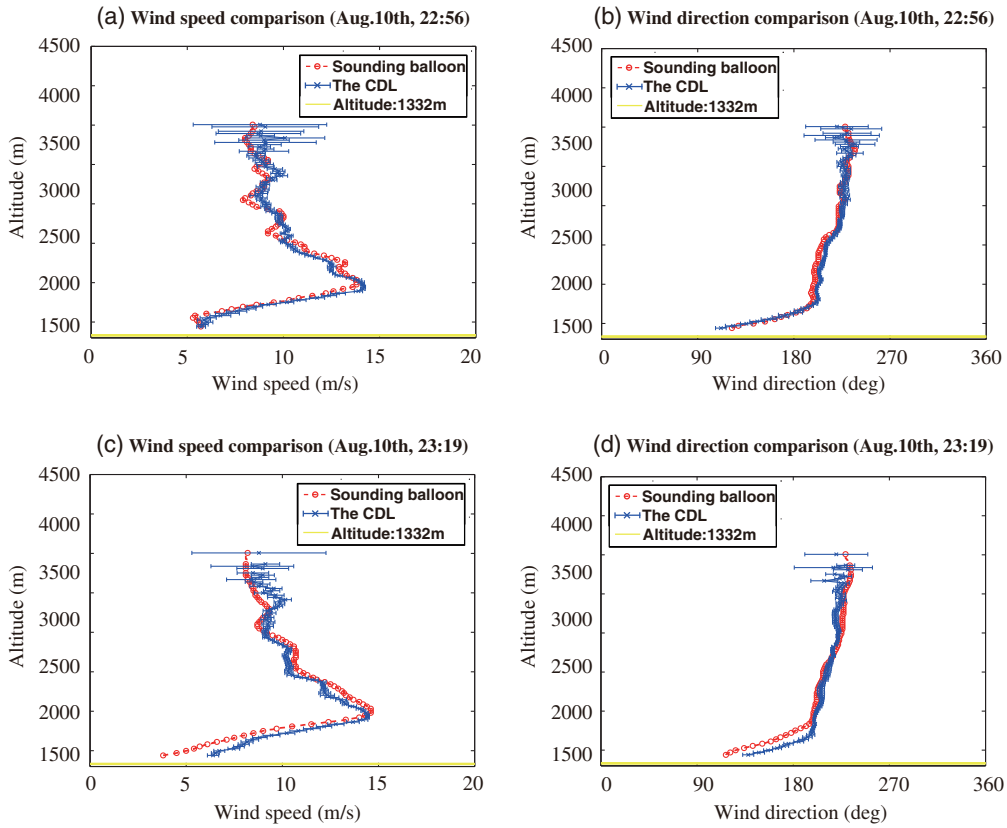

Fig. 5 Comparison of horizontal wind velocity between the CDL (blue cross, with 10-min error bar) and sounding balloon (red dot). (a) and (b) The horizontal wind speed comparison and horizontal wind direction comparison during the ascent period of sounding balloon, respectively. (c) and (d) The horizontal wind velocity comparison during the descent period of sounding balloon.

affected by weak signal regime, atmospheric turbulence, etc. At the end of descent period, the discrepancy of wind velocity measured by sounding balloon (dot) and the CDL (cross) mainly ascribes to the measured wind field by two sensors. The sounding balloon flies away (about 10 km) as time goes by (after 19 min).

Comparison of horizontal wind velocity is shown in Fig. 6. Comparison of wind direction shown in the first row shows good accordance in most situations. In the second row, wind speed

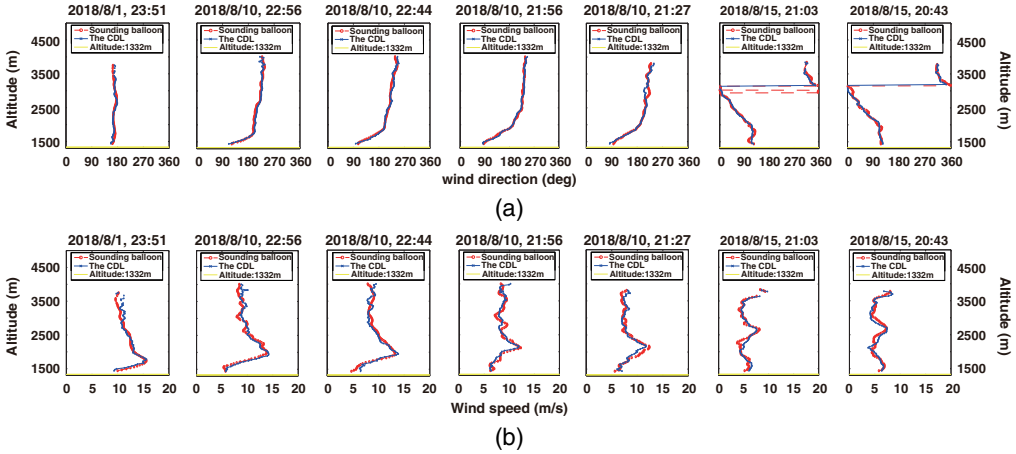

Fig. 6 Comparison of horizontal wind velocity detected by CDL and sounding balloon. Comparison of (a) wind direction and (b) wind speed.

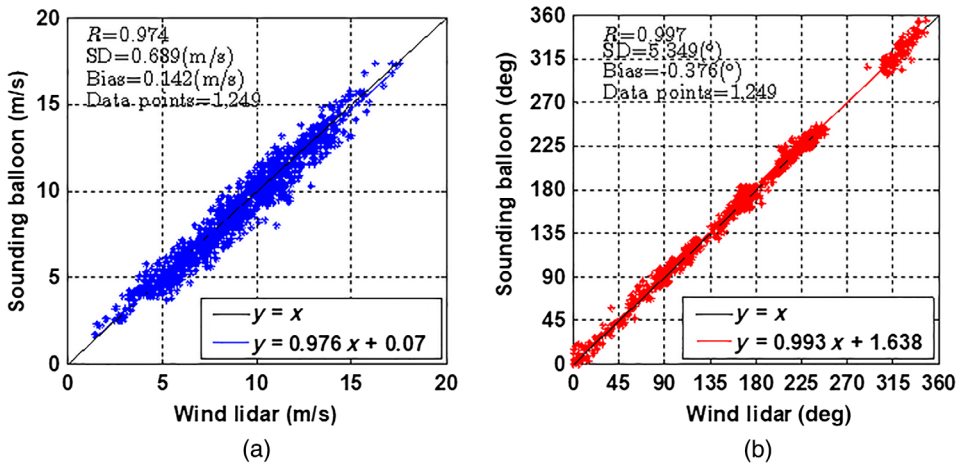

Fig. 7 Horizontal wind velocity correlation of (a) wind speed and (b) direction on August 2018.

detected by two instruments shows similar tendency, and a divergence of about 1 to 2 m/s of 30-s averaged wind speed is found between the CDL and sounding balloon.

Linear correlation and numerous analyses of wind velocity are shown in Fig. 7. The linear fits of scattering points fluctuate about the line $y = x$. In combination with the correlation coefficient (R: 0.974 of wind speed and 0.997 of wind direction), an obviously positive correlation between the wind dataset of the CDL and that of sounding balloon is displayed in Fig. 7. The typical discrepancy of wind speed and wind direction between the two systems is about 0.7 m/s and 5.3 deg, respectively. Discarding the accidental error of sounding balloon of manual operation, the little bias of wind speed and direction is mainly affected by the intermediate frequency offset and due to north deflection of the CDL, respectively.

To our knowledge, the routine sounding balloon system has an accuracy of horizontal wind speed <1 m/s and wind direction within 5 deg in the lower troposphere.[25,31] During the intercomparison experiments in Jingbian, China, as the reference with time period of 30 s, vertical resolution of sounding balloon is better than 150 m. Averaging time period shorter than 2 min cannot reach sufficiently smooth;[25] therefore, 30-s averaged wind velocity usually occurs natural turbulent fluctuations of wind field. By comparing the wind velocity measured by different principles, the good agreement of experimental results could testify the accuracy of the CDL with acceptable limits.

3.3 *Sample of Continuous Wind-Profile Measurements of the CDL*

In August 2018, the field observation was launched and the continuous 3-D wind field datasets were obtained by the CDL. A measured continuous wind profiles were sampled and shown in Fig. 8. The maximum detection altitude on that day was 4400 m (local altitude: 1332 m), which provided sufficient detection range in the field experiments.

According to the horizontal wind speed profiles [Fig. 8(a)], the horizontal wind speed was >5 m/s in most of the time. From 20:00 to 24:00, horizontal wind speed was intensive in range of 1500 to 2500 m. Meanwhile, the horizontal wind direction profiles [Fig. 8(b)] revealed that the horizontal wind direction was steady at that night.

In the vertical wind velocity profiles [Fig. 8(c)], sign setting on this ground-based system leads to positive relative speeds for downward winds or vice versa. Throughout the measurement period, vertical wind velocity is mostly positive corresponding to downdraft. Interestingly, the vertical wind velocity changes quickly and frequently from 16:00 to 19:00 and becomes relatively steady on that night.

4 Conclusion

Wind velocity measured by the pulsed CDL shows good agreement with that of collocated wind lidar and sounding balloon in field experiments. Time sequence and height positions of the CDL

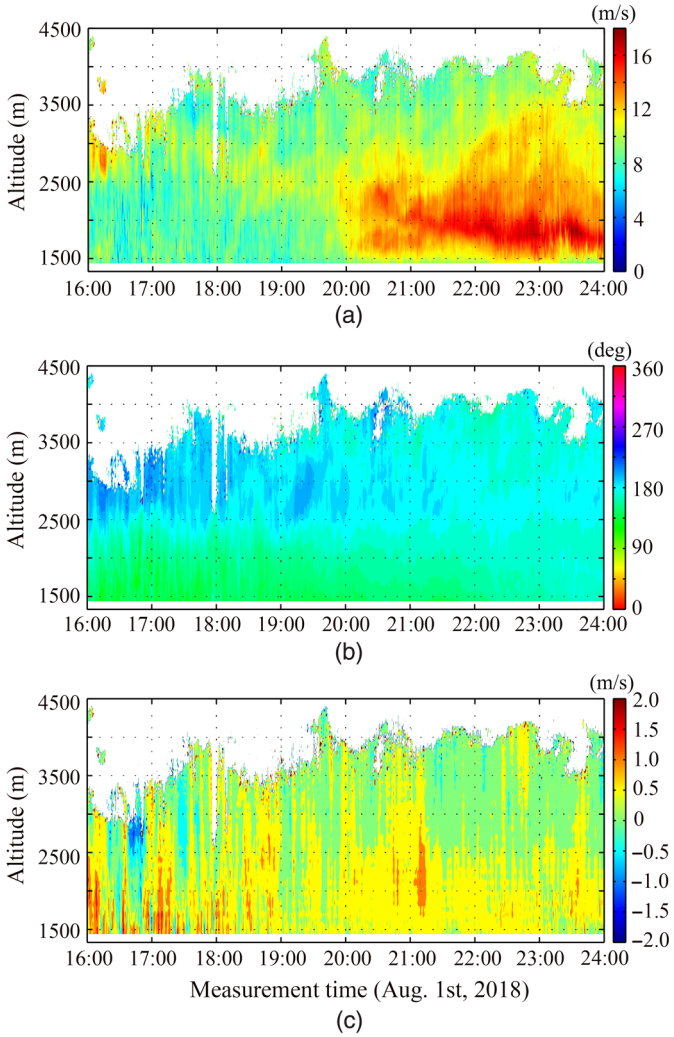

Fig. 8 Continuous wind profiles measurement by the ground-based CDL (local altitude: 1332 m) on August 1, 2018. (a) Horizontal wind speed profiles, (b) horizontal wind direction profiles, and (c) vertical wind velocity profiles.

are first calibrated by the collocated lidar. As compared with collocated wind lidar, the 10-min level discrepancy of horizontal wind speed, direction, and vertical wind velocity are 0.164 m/s, 1.719 deg, and 0.07 m/s, respectively. In the intercomparison experiments with sounding balloon, the 30-s level discrepancy of horizontal wind speed and direction is nearly 0.7 m/s and 5.3 deg, respectively. The CDL system demonstrates the stability and reliability in field experiments.

Acknowledgments

This work was supported by the National Key Research and Development Program of China under Grant No. 2017YFF0104600 and the Pre-Research Project of Civilian Space under Grant No. D040103. The authors are grateful for the collocated wind lidar Molas B300 provided by Move laser Co., Ltd. They also declare no conflicts of interest.

References

1. S. Wu et al., "Wind turbine wake visualization and characteristics analysis by Doppler lidar," *Opt. Express* **24**(10), A762–A780 (2016).

2. T. Fujii and T. Fukuchi, *Laser Remote Sensing*, CRC Press, Taylor & Francis Group, Boca Raton (2005).
3. C. Wang et al., "1.5 μm polarization coherent lidar incorporating time-division multiplexing," *Opt. Express* **25**(17), 20663–20674 (2017).
4. L. Bu et al., "All-fiber pulse coherent Doppler lidar and its validations," *Opt. Eng.* **54**(12), 123103 (2015).
5. T. Ando et al., "All-fiber coherent Doppler lidar for wind sensing," in *MRS Online Proc. Lib. Arch.*, Vol. 1076 (2008).
6. S. Rahm and I. Smalikho, "Aircraft wake vortex measurement with airborne coherent Doppler lidar," *J. Aircr.* **45**(4), 1148–1155 (2008).
7. S. Wu, X. Zhai, and B. Liu, "Aircraft wake vortex and turbulence measurement under near-ground effect using coherent Doppler lidar," *Opt. Express* **27**(2), 1142–1163 (2019).
8. I. N. Smalikho and V. A. Banakh, "Measurements of wind turbulence parameters by a conically scanning coherent Doppler lidar in the atmospheric boundary layer," *Atmos. Meas. Tech.* **10**(11), 4191–4208 (2017).
9. V. A. Banakh and I. N. J. R. S. Smalikho, "Lidar estimates of the anisotropy of wind turbulence in a stable atmospheric boundary layer," *Remote Sens.* **11**(18), 2115 (2019).
10. T. J. Kane et al., "Coherent laser radar at 1.06 μm using Nd:YAG lasers," *Opt. Lett.* **12**(4), 239–241 (1987).
11. U. N. Singh et al., "Twenty years of Tm:Ho:YLF and LuLiF laser development for global wind and carbon dioxide active remote sensing," *Opt. Mater. Express* **5**(4), 827–837 (2015).
12. X. Zhang et al., "Single-frequency polarized eye-safe all-fiber laser with peak power over kilowatt," *Appl. Phys. B* **115**(1), 123–127 (2014).
13. S. Abdelazim et al., "Development of All-Fiber Coherent Doppler Lidar System for Wind Sensing," in *15th Symp. Meteorological Observation Instrumentation*, American Meteorological Society, Boston (2010).
14. A. Joshi et al., "Coherent optical receiver system with balanced photodetection," *Proc. SPIE* **6243**, 62430E (2006).
15. X. Rui et al., "Adaptive iteratively reweighted sine wave fitting method for rapid wind vector estimation of pulsed coherent Doppler lidar," *Opt. Express* **27**(15), 21319–21334 (2019).
16. C. Wang et al., "Spatial resolution enhancement of coherent Doppler wind lidar using joint time-frequency analysis," *Opt. Commun.* **424**(1), 48–53 (2018).
17. J. Liu et al., "All-fiber airborne coherent Doppler lidar to measure wind profiles," *EPJ Web Conf.* **119**, 10002 (2016).
18. B. W. Barnes et al., "Wind measurements with high energy 2 micron coherent Doppler lidar," in *22nd Int. Laser Radar Conf.*, Matera, Italy (2004).
19. G. D. Emmitt, "Comparison of GWOLF and VALIDAR Doppler lidar measurements," in *2nd Symp. Lidar Atmos. Appl.* (2005).
20. H. Inokuchi, H. Tanaka, and T. Ando, "Development of an onboard Doppler lidar for flight safety," *J. Aircr.* **46**(4), 1411–1415 (2009).
21. S. Kameyama et al., "Compact all-fiber pulsed coherent Doppler lidar system for wind sensing," *Appl. Opt.* **46**(11), 1953–1962 (2007).
22. K. Asaka, T. Yanagisawa, and Y. Hirano, "1.5 μm eye-safe coherent lidar system for wind velocity measurement," *Proc. SPIE* **4153**, 321–328 (2001).
23. J. P. Cariou et al., "Long range scanning pulsed coherent lidar for real time wind monitoring in the planetary boundary layer," in *Proc. 16th Conf. Coherent Laser Radar* (2011).
24. X. Zhai et al., "Shipborne wind measurement and motion-induced error correction of a coherent Doppler lidar over the Yellow Sea in 2014," *Atmos. Meas. Tech.* **11**(3), 1313–1331 (2018).
25. World Meteorological Organization, *WMO Guide to Meteorological Instruments and Methods of Observation*, p. 681, Secretariat of the World Meteorological Organization, Geneva, Switzerland (2008).
26. E. Päschke, R. Leinweber, and V. Lehmann, "A one year comparison of 482 MHz radar wind profiler, RS92-SGP radiosonde and 1.5 μm Doppler lidar wind measurements," *Atmos. Meas. Tech. Discuss* **7**(11), 11439–11479 (2014).
27. G. J. Koch et al., "Field testing of a high-energy 2-μm Doppler lidar," *J. Appl. Remote Sens.* **4**(1), 043512 (2010).

28. F. Chouza et al., "Retrieval of aerosol backscatter and extinction from airborne coherent Doppler wind lidar measurements," *Atmos. Meas. Tech.* **8**(7), 2909–2926 (2015).
29. W. Li and Y. C. Zhang, "The wind-finding performance evaluation of GFE(L)1 secondary radar," *J. Chengdu Univ. Inf. Technol.* **26**(1), 91–97 (2011).
30. J. Nash et al., "WMO intercomparison of high quality radiosonde systems, Yangjiang, China, 12 July–3 August 2010," Report No. 107, World Meteorological Organization (2011).
31. C. M. Administration, "Conventional upper-air weather detection specification," in *China Meteorological Administration, Conventional upper-air weather detection specification*, China meteorological Press, Beijing(2010).

Heng Liu received his BS degree from School of Science of Nanchang University in 2017, and he is a candidate for an MS degree in Optics Engineering in the University of Chinese Academy of Sciences. He is ready for research in laser transmitter and coherent Doppler lidar system.

Xiaopeng Zhu completed his PhD from the University of Chinese Academy of Sciences in 2011. He is an associate professor at Shanghai Institute of Optics and Fine Mechanics, Chinese Academy of Sciences. His research interest is in Doppler wind lidar.

Jiqiao Liu completed his PhD from the University of Chinese Academy of Sciences in 2006. He is a professor at Shanghai Institute of Optics and Fine Mechanics, Chinese Academy of Science. He has expertise in Doppler wind lidar, Integrated Path Differential of Absorption lidar and airborne Aerosol and Cloud Detection lidar.

Xiaolei Zhu completed his PhD from the Chinese University of Hong Kong in 2001. He has expertise in solid-state lasers and various laser application systems. He is the director of a research team in Shanghai Institute of Optics and Fine Mechanics, Chinese Academy of Sciences.

Weibiao Chen is a professor at Shanghai Institute of Optics and Fine Mechanics, Chinese Academy of Sciences and leader of the space laser and applied system group. His research interest is in laser remote sensing application and all-solid laser technology.

Biographies of the other authors are not available.